Anal. Chem. **2009,** *81,* 4762–4769

Fully Integrated Three-Dimensional Electrodes for Electrochemical Detection in Microchips: Fabrication, Characterization, and Applications

Rekha S. Pai,*,† Kevin M. Walsh,† Mark M. Crain,† Thomas J. Roussel, Jr.,‡ Douglas J. Jackson,† Richard P. Baldwin,§ Robert S. Keynton,‡ and John F. Naber†

Departments of Electrical and Computer Engineering, Bioengineering, and Chemistry, University of Louisville, Louisville, Kentucky 40292

A scalable and rather inexpensive solution to producing microanalytical systems with "on-chip" three-dimensional (3D) microelectrodes is presented in this study, along with applicability to practical electrochemical (EC) detection scenarios such as preconcentration and interferant removal. This technique to create high-aspect-ratio (as much as 4:1) gold microstructures in constrained areas involved the modification of stud bump geometry with microfabricated silicon molds via an optimized combination of temperature, pressure, and time. The microelectrodes that resulted consisted of an array of square pillars ~18 μm tall and 20 μm wide on each side, placed at the end of a microfabricated electrophoresis channel. This technique increased the active surface area of the microelectrodes by as much as a factor of 50, while mass transfer and, consequently, preconcentration collection efficiencies were increased to ~100%, compared to ~30% efficiency for planar nonmodified microelectrodes (samples that were used included the neurotransmitters dopamine and catechol). The 3D microelectrodes were used both in a stand-alone configuration, for direct EC detection of model catecholamine analytes, and, more interestingly, in dual electrode configurations for EC sample processing prior to detection downstream at a second planar electrode. In particular, the 3D electrodes were shown to be capable of performing coulometry or complete (100%) redox conversion of analyte species over a wide range of concentrations, from 4.3 μM to 4.4 mM, in either plug-flow or continuous-flow formats.

Fully integrated portable microsystems for use in remote or unsupervised monitoring can be easily realized using on-chip electrochemical (EC) detection in which the sense/detection electrodes are integrated directly onto the microchip.[1−13] In addition to its inherent miniaturization potential, this approach offers attractive sensitivity, with detection limits in the nanomolar range, independence from optical path length or sample turbidity, low cost, and, above all, the flexibility to customize electrode shape, size, geometry, and material based on the application.[2,9−11]

Practical realizations of this EC detection approach such as preconcentration, catalysis, and binding wherein trace amounts of molecules must be trapped and/or completely reacted in the presence of background interferants can be achieved by high-surface-area electrodes. Furthermore, the Faradaic EC detection equations suggest that a significant sensitivity enhancement in the diffusion-limited detection current can be obtained by increasing the area and/or optimizing the electrode shape, so that more of the analyte comes into contact with and is reduced/oxidized at the sensing electrode surface.[14−16] Despite microfabrication conferring the ability to vary electrode geometry with micrometer-

* To whom correspondence should be addressed. Currently with the U.S. Naval Research Laboratory (NRL), Code 6365—Materials and Sensors, Washington, DC 20375-5345. Tel.: 202-767-6302. Fax: 202-767-2087. E-mail: rekha.pai@nrl.navy.mil.

† Department of Electrical and Computer Engineering.

‡ Department of Bioengineering.

§ Department of Chemistry.

(1) Jiang, Y.; Wang, P.-C.; Locascio, L. E.; Lee, C. S. *Anal. Chem.* **2001**, *73*, 2048–2053.

(2) Wang, J.; Tian, B.; Sahlin, E. *Anal. Chem.* **1999**, *71*, 5436–5440.

(3) Hilmi, A.; Luong, J. H. T. *Electrophoresis* **2000**, *21*, 1395–1404.

(4) Wang, J.; Pumera, M.; Chatrathi, M. P.; Escarpa, A.; Musameh, M.; Collins, G.; Mulchandani, A.; Lin, Y.; Olsen, K. *Anal. Chem.* **2002**, *74*, 1187–1191.

(5) Wang, J.; Zima, J.; Lawrence, N. S.; Chatrathi, M. P.; Mulchandani, A.; Collins, G. *Anal. Chem.* **2004**, *76*, 4721–4726.

(6) Verpoorte, E.; De Rooij, N. F. *Proc. IEEE* **2003**, *91*, 930–950.

(7) Roulet, J.-C.; Volkel, R.; Herzig, H. P.; Verpoorte, E.; De Rooij, N. F.; Dandliker, R. *Anal. Chem.* **2002**, *74*, 3400–3407.

(8) Pasas, S. A.; Fogarty, B. A.; Huynh, B. H.; Lacher, N. A.; Carlson, B.; Martin, R. S.; Vandaveer, W. R.; Lunte, S. M. In *Separation Methods in Microanalytical Systems*; Kutter, J. P., Fintschenko, Y., Eds.; Marcel Dekker: New York, 2004.

(9) Baldwin, R. P.; Roussel, T. J., Jr.; Crain, M. M.; Bathlagunda, V.; Jackson, D. J.; Gullapalli, J.; Conklin, J. A.; Pai, R.; Naber, J. F.; Walsh, K. M.; Keynton, R. S. *Anal. Chem.* **2002**, *74*, 3690–3697.

(10) Lacher, N. A.; Garrison, K. E.; Martin, R. S.; Lunte, S. M. *Electrophoresis* **2001**, *22*, 2526–2536.

(11) Wang, J. *Talanta* **2002**, *56*, 223–231.

(12) Jackson, D. J.; Naber, J. F.; Roussel, T. J., Jr.; Crain, M. M.; Walsh, K. M.; Keynton, R. S.; Baldwin, R. P. *Anal. Chem.* **2003**, *75*, 3643–3649.

(13) Keynton, R. S.; Roussel, T. J., Jr.; Crain, M. M.; Jackson, D. J.; Franco, D. B.; Naber, J. F.; Walsh, K. M.; Baldwin, R. P. *Anal. Chim. Acta* **2004**, *507*, 95–105.

(14) Heineman, W. R.; Kissinger, P. T. In *Laboratory Techniques in Electroanalytical Chemistry*, 2nd Edition; Kissinger, P. T., Heineman W. R., Eds.; Marcel Dekker: New York, 1996; pp 51−126.

(15) Bard, A. J.; Faulkner, L. R. *Electrochemical Methods: Fundamentals and Applications*, 1st Edition; John Wiley and Sons: New York, 1980; pp 370−428.

(16) Toth, K.; Stulik, K.; Kutner, W.; Feher, Z.; Lindner, E. *Pure Appl. Chem.* **2004**, *76*, 1119–1138.

(17) Wang, J.; Pumera, M.; Chatrathi, M. P.; Rodriguez, A.; Spillman, S.; Martin, R. S.; Lunte, S. M. *Electroanalysis* **2002**, *14*, 1251–1255.

(18) Martin, R. S.; Gawron, A. J.; Fogarty, B. A.; Regan, F. B.; Dempsey, E.; Lunte, S. M. *Anal. Chem.* **1999**, *71*, 251–255.

(19) Gawron, A. J.; Martin, R. S.; Lunte, S. M. *Electrophoresis* **2001**, *22*, 242–248.

10.1021/ac9002529 CCC: $40.75
Published on Web 05/21/2009

level accuracy, there has been only one instance in the published literature so far where a nonplanar electrode has been utilized in lab-on-a-chip (LOC) systems.[17] Wang et al.[17] described this end-channel on-chip detection scheme where a screen-printed thick-film carbon electrode (called "flow-onto/flow-by" hybrid by the authors) was used. Because the electrode thickness of 40 μm was slightly higher than the 35-μm-wide channels etched into the polydimethylsiloxane (PDMS) microchips, this allowed the sample to flow from the channel onto the side of the electrode (acting as a "wall") and later flow onto the top surface of the sensing electrode. The limit of detection (LOD) for catechol on this microchip was 280 nM, which is lower than the 610 nM value that was reported by the same group for "flow-onto only" screen-printed carbon detectors on glass devices[2] and for similar PDMS-based planar carbon working electrode LOC systems presented by Lunte and co-workers.[18,19] The authors attributed the improvement in LODs, good sensitivity, and low noise level to the effective isolation from the separation voltage, and to the enhanced mass transport of analyte caused by the combined flow-onto/flow-by flux, i.e., the increased active surface area.

A relatively simpler LOC device was used by Liu et al.[20] to investigate factors such as areas of electrodes and materials. In this microchip, copper, gold, and platinum wires 25−50 μm in diameter were introduced on-chip via an electrode alignment channel placed orthogonal to the direction of flow. Increased collection efficiencies of 90% and LODs of 100 nM for dopamine were achieved using the larger-diameter (50 μm) platinum wire, which were the lowest values reported for end-channel detection in microchips. However, despite the exact placement of the wire electrodes, with respect to the capillary exit, collection efficiencies and elution times for the neutral catecholamines varied by as much as 30% and 40−60 s, respectively.

In summary, although theory and these two papers predict benefits in using high-surface-area electrodes for EC detection, practical restrictions are imposed by the inherently two-dimensional (2D) nature of traditional photolithography. Lithography, sputtering, and etching processes that are currently applied in the fabrication of LOC systems originated from the integrated circuit (IC) manufacturing industry. Consequently, they produce low-aspect-ratio structures, are often limited to the use of materials such as silicon and metals, and have limited tolerances to nonplanar topography. Alternative high-aspect-ratio strategies such as stereolithography, electroplating, and LIGA are difficult to achieve in constrained areas (e.g., microchannels), in addition to being expensive. In this study, a nonconventional micromachining technique capable of producing three-dimensional (3D) microstructures for use as electrodes in confined channels and/or reservoirs has been developed to realize higher sensitivity and lower LODs in LOC systems.

In addition, an effective way of increasing the efficacy of a traditional EC detection system is through the use of dual-series electrodes, where two working electrodes are oriented in series, with respect to the flow axis.[21,22] This dual detection configuration is especially practical as shown by Schieffer when the upstream electrode is a coulometric high-surface-area electrode that is capable of oxidizing/reducing all interferants, so that the analyte of interest can be detected with increased selectivity at the second electrode. Several potential applications such as toxic waste monitoring and forensic analysis could benefit, because of the enhancement in selectivity, peak identification, and high gain detection afforded by this configuration. This is particularly significant, because this can be accomplished with a mixed sample that has a volume of only a few nanoliters and contains an attomolar amount (10^{-18}) of analyte within a matter of minutes.

Although a handful of papers have been published on planar dual-series electrode microchips for peak identification,[19,23,24] little attention has been given to realizing practical applications such as (a) the development of upstream electrodes that are capable of 100% collection efficiency (i.e., coulometric-amperometric detection configurations or sample cleanup platforms[25]); (b) preconcentration at the first electrode and subsequent detection at the second detector, to enhance signal sensitivity and selectivity for small sample sizes;[26] and (c) on-chip derivatization schemes for inherently nonelectroactive substances such as peptides, thiols, and disulfides as in conventional CE. Some of our efforts in this regard are presented in this study. More importantly, a comparison of LOC systems with planar and 3D electrode configurations has been performed to demonstrate the latter's efficacy.

EXPERIMENTAL SECTION

Microchip Fabrication. The CE/EC microchip (see Figure 1) was fabricated from thermally bonded soda−lime glass, where the top half contained the etched channels and access ports, while all the electrodes were patterned on the bottom substrate.[9,12,13] The anisotropic CE channels were etched using 6:1 buffered oxide etch (BOE) at room temperature to a depth of ~22 μm ± 0.7 μm, and widths of 80 μm at the top and 50 μm at the bottom (for an average width of 65 μm). Access to the channels was created by drilling four reservoirs in the glass; these reservoirs are named according to their functions: sample, EC detection, waste, and buffer. A glass "shelf", as depicted in Figure 1b, was formed by drilling the EC detection reservoir ~450 μm away from the capillary exit.

The bottom substrate contained 11 electrodes: 4 CE drive electrodes (one in each of the reservoirs) and 7 EC electrodes (of which, 6 crescent-shaped electrodes (i.e., three pairs) are working/sense electrodes, as illustrated in Figure 2, and the remaining electrode functions as a reference (not shown in the figure). In the large-surface-area dual-series configurations, the electrode pair closest to the capillary exit (W1AB) was transformed to be three-dimensional (3D), while the other pairs remained planar. The pseudo-reference and CE electrodes were patterned as metal strips 2.2 mm wide and 6.9 mm long that are located far from the channels to minimize bubble generation caused by hydrolysis of the buffer solution. All the electrodes were formed by a sequence of steps: photolithographic "lift-off" to define the dimensions, and BOE etch to define the electrode pattern, followed by sputtering

(20) Liu, Y.; Vickers, J. A.; Henry, C. S. *Anal. Chem.* **2004**, *76*, 1513–1517.
(21) Roston, D. A.; Kissinger, P. T. *Anal. Chem.* **1982**, *54*, 429–434.
(22) Schieffer, G. W. *Anal. Chem.* **1980**, *52*, 1994–1948.
(23) Martin, R. S.; Gawron, A. J.; Lunte, S. M.; Henry, C. S. *Anal. Chem.* **2000**, *72*, 3196–3202.
(24) Martin, R. S.; Gawron, A. J.; Fogarty, B. A.; Regan, F. B.; Dempsey, E.; Lunte, S. M. *Analyst* **2001**, *126*, 277–280.
(25) Roussel, T. J.; Pai, R. S.; Crain, M. M.; Jackson, D. J.; Sztaberek, L.; Walsh, K.; Naber, J. F.; Baldwin, R. P.; Keynton, R. S. *IEEE/EMBS Conf. Microtechnol. Med. Biol.* **2006**, *4th*, 233–235.
(26) Pai, R. S.; Roussel, T. J.; Crain, M. M.; Jackson, D. J.; Baldwin, R. P.; Keynton, R. S.; Naber, J. F.; Walsh, K. M. *IEEE/EMBS Conf. Microtechnol. Med. Biol.* **2005**, *3rd*, 18–21.

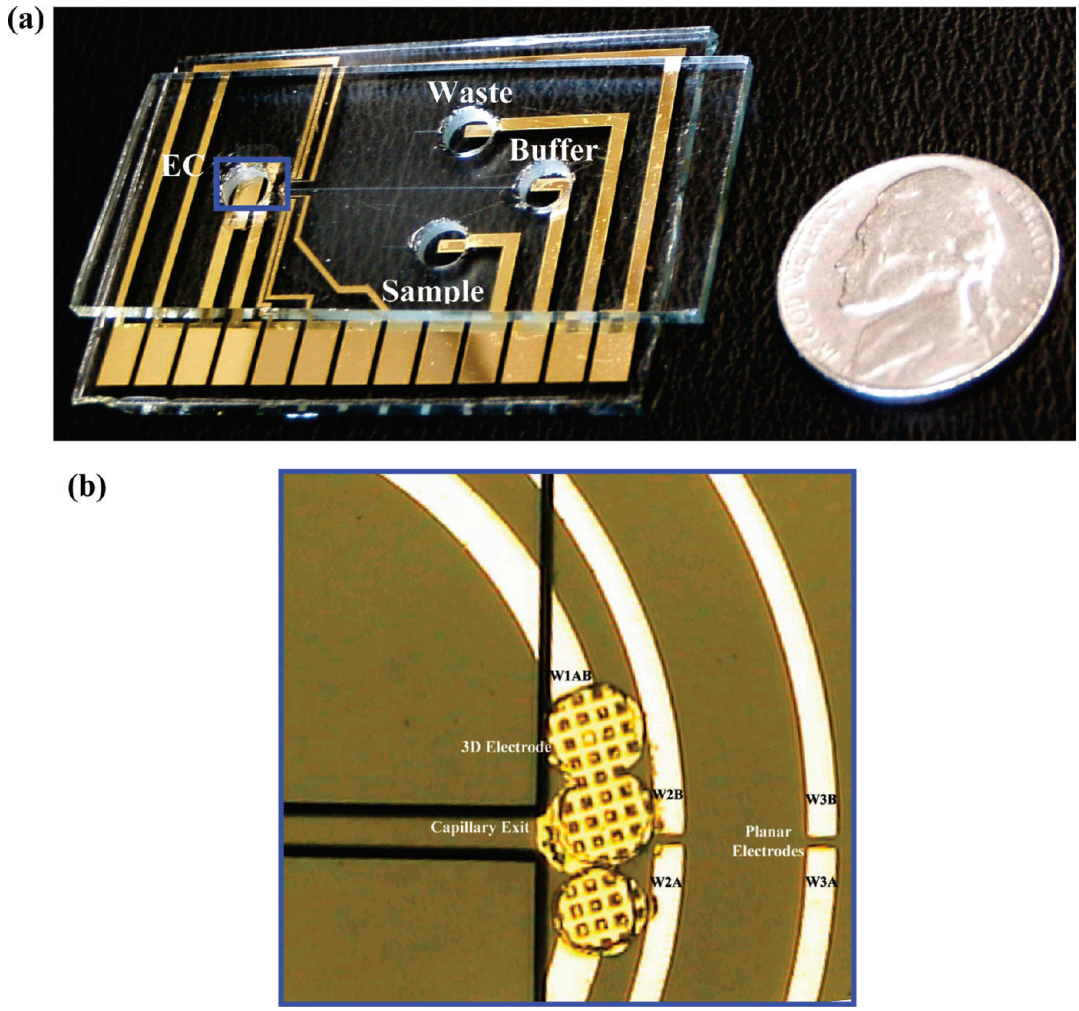

Figure 1. Photograph of (a) the entire CE/EC device and (b) a close-up view of the end-channel EC detection setup (top view).

for the electrodes (a 300-nm-thick layer of gold with a 30-nm-thick adhesion layer of tungsten).

At this point, the two halves of the microchip are ready for thermal bonding to form the control group microchips with completely planar electrode configurations. In addition, the 3D LOC design had the same fabrication methodology, except that the first pair of planar electrodes was converted to a high-surface-area microelectrode system. A trio of stud bumps was placed in a semicircle at the center of the radial pattern that forms the first working electrode pair, as shown in Figure 2a. The ball bumping was performed with 1-mil gold wire in a fine-pitch capillary (414FB, with a capillary diameter of 1.5 mil) on a K&S 4524 digital wire bonder, using the following parameters: power, 4.19; force, 5.4; ball, 4.0; tail, 3.2; time, 6.6; and chuck temperature, 150 °C. Care was taken during the ball bumping placement to ensure that the stud bumps span the first pair of electrodes to form one working electrode while not touching—and, thus, shorting—the second set of working electrodes. The three gold bumps were then "coined", i.e., the top surface was flattened as in Figure 2b, using a flat piece of a silicon wafer on a Finetech "Pico" flip chip bonder. A force of 15 N that was applied for 45 s with die and chuck temperatures of 200 °C were determined to be the ideal conditions for the flattening procedure. In the last step, the gold stud bumps were transformed to a "forest" of finger-shaped microstructures by imprinting them with microfabricated high-aspect-ratio silicon molds. The 50-μm-deep molds were fabricated using standard ultraviolet (UV) photolithography and deep reactive ion etching (DRIE). A monolayer of an antistiction agent (perfluorooctyltrichlorosilane) was evaporated onto the micromold (20 μm square each, with a separation of 10 μm), which was then aligned to the three coined gold stud bumps and the inverse of the pattern was imprinted (Figure 2c). This imprinting process was accomplished on a Finetech "Pico" flip chip bonding system with optimal parameters to obtain microelectrodes ~20 μm high; die and chuck temperature, 200 °C; time, 45 s; and force, 22 N. Metrology was conducted on the 3D micropillars (Figure 2d), using a SEM and WYKO profilometer.

In the next step, the two patterned glass substrates—one containing the electrodes and the other containing microchannels—were aligned under an optical microscope. A thin film of water that was between the two substrates enabled slight, careful relative movement without causing damage to the electrodes. The distance from the capillary exit to the 3D microelectrode lead edge was adjusted to be ~40−100 μm, while ensuring that all the working electrodes were situated below the "shelf", as depicted in Figure 1b.

After satisfactory alignment, a steady pressure was applied and maintained on the chips using fingertips while drying with nitrogen, to squeeze out excess water. This step led to a lightly bonded chip that was sandwiched between blocks of alumina and transferred to a tube furnace for thermal bonding. An Inconel

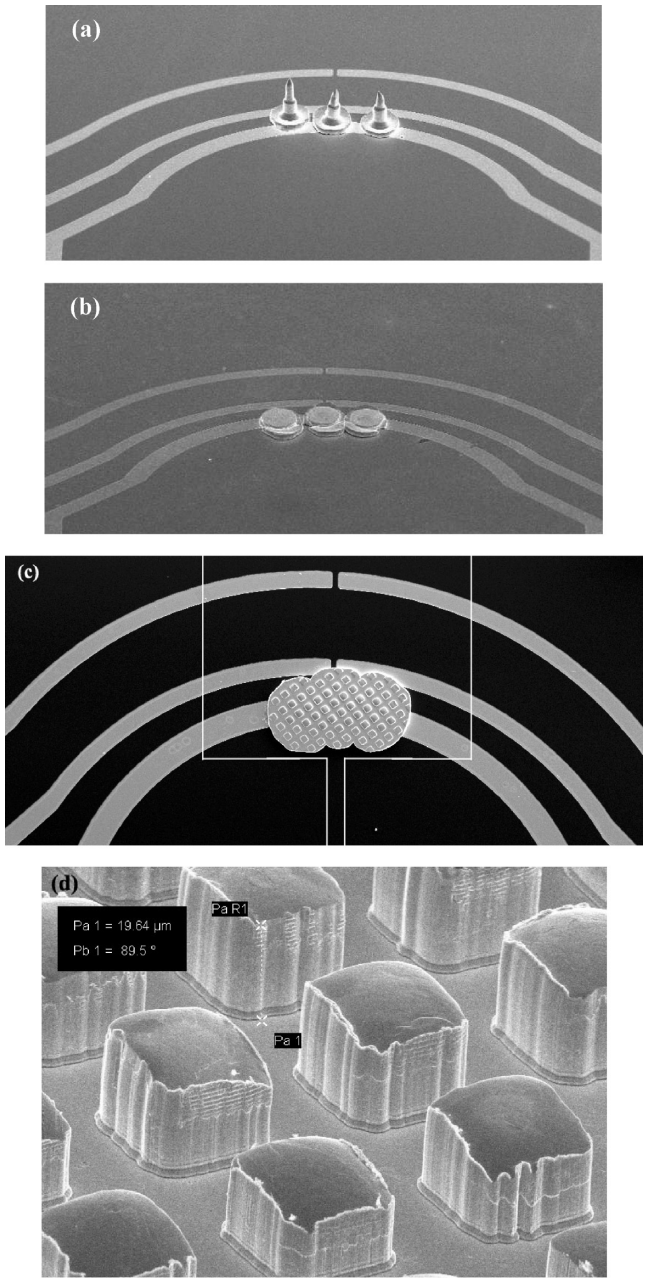

Figure 2. Scanning electron microscopy (SEM) images obtained at different stages of the process: (a) the gold stud bumps, (b) coined stud bumps, (c) three-dimensional (3D) microelectrodes, and (d) closeup of the final electrodes.

weight that was placed atop the entire assembly was used to apply an even pressure of 50 g/cm^2 over the entire chip. The bonding sequence involved a ramp of 3 °C/min to 635 °C, followed by a 30-min plateau and ending with a slow cool to room temperature (argon gas flow = 10 mL/min).

Electronics. The main instrumentation used for control and operation of the LOC system was a miniaturized, custom-built electronics unit that consisted of a dual-source high-voltage power supply (HVPS), interface circuit, and amperometric EC detection module. A detailed description including the HVPS and EC detection circuitry for a three-electrode system (i.e., working, reference, and counter) has been previously reported.[18] In this study, a selectable-gain transimpedance amplifier and a potentiostat were added, allowing for dual EC detection.

Reagents. All chemicals were purchased from commercial sources (Sigma−Aldrich Co.) and were used as received, without further purification. The background electrolyte solution for all the neurotransmitter experiments was a 0.02 M pH 6.5 sodium phosphate buffer. Analyte solutions of the neurotransmitters dopamine (MW = 189.64) and catechol (MW = 110.11), in appropriate concentrations (generally 1−2 mM), were prepared fresh daily by dissolving them in stock solutions of the phosphate buffer.

RESULTS AND DISCUSSION

Microchip Design. Figure 1a shows a photograph of a typical CE/EC device with the gold electrodes, while the optical and SEM micrographs in Figures 1b and 2c provide a detailed view that shows, more precisely, the location, size, configuration, and orientation of the channels and electrodes in the LOC chips. Note that, although Figures 1b and 2c show gold microelectrodes that extend beyond the first electrode pair onto the second (possibly shorting the pair), this was not the case with the final devices. Before bonding, resistances were measured to ensure that the adjacent electrode pairs were not connected.

Critical dimensions of the 3D electrodes in the LOC system were measured using profilometry, and each of the finger-shaped microstructures was determined to be 18 ± 1 μm tall, with each side measuring 20 μm. This design of the 3D microelectrodes was chosen keeping in mind the limited amount of gold available in the stud bump (20 ± 1 μm high and 105 ± 5 μm in diameter after flattening) and the height of the channel, while maximizing the surface area, although other templates could very well have been used.

Slight variations do exist from chip to chip, because critical steps such as placement of the stud bumps adjacent to each other, mechanical coining, micromolding, the drilling of reservoirs to create a "shelf", as well as final optical alignment, are dependent on the skill of the operator. Some characteristics or steps that were important in the construction of an acceptable chip, and the associated issues, included shelf width, 3D microelectrode fabrication, working electrode position, and bonding.

Shelf Widths. In our earlier work,[9] we discussed the importance of a "shelf" of glass, which is created by drilling the detection reservoir away from the edge of the channel exit. This "shelf" effectively confined diffusion of the analyte plug in the *z*-dimension until the analyte flows past all the working electrodes, consequently increasing the mass transfer. Even with the best efforts, this critical step was difficult to control, with resulting detection reservoirs having slight chipping and shelf widths of 400−960 μm.

Three-Dimensional (3D) Microelectrode Fabrication. Central to this methodology is the formation of the stud bump and its accurate placement at the center of the fluid flow on the first electrode, while avoiding contact with the second electrode pair located just 45 μm away (see Figure 1b). The close spacing of the bumps also caused some interference by the bonder capillary with the first stud bump when placing the adjacent bump. During processing, this issue was mitigated to some extent with the use of finer-pitch capillaries to place smaller stud bumps offset from the electrodes. However, the spread in bump width due to the coining and micromolding steps was not predictable. A few factors that were vital to the formation of 3D microelectrodes were good adhesion between the planar traces/glass substrate/stud bump

interfaces, the cleanliness of the micromolds used, and perhaps, more importantly, performing the imprinting process within a day or two of evaporating a monolayer of the antistiction agent. Ignoring any of these factors meant that the stud bumps and the planar gold trace would delaminate upon contact by the mold.

Working Electrode Position. It was determined early on that maximization of the EC detection currents (sharp peaks with no band-broadening) required placement of the EC working electrode close to the CE channel exit.[9,13] In this LOC system, the triplet of stud bumps were placed ~60−100 μm away from the capillary exit, as a compromise, because of the higher background currents that result from the CE fields being further aggravated by the increased surface area of the electrodes. The challenge in this process lay in alignment of the two components of the microchip: the top half with the ~23-μm-high etched CE channels and the bottom substrate containing the ~20-μm-high 3D microelectrodes.

Bonding. Thermal bonding presented problems with chips not bonding well at low temperatures and the glass unsupported "shelf" collapsing at ~645 °C. The solution was sandwiching the aligned microchips between alumina, to ensure uniform thermal conduction while providing support during the thermocompression bonding at 635 °C. A total of 11 chips with the 3D microelectrodes and 3 planar LOC systems were successfully fabricated for this study, using this methodology.

Analytical Parameters. The first characterization experiment was a comparison of the current response at the trio of modified stud bumps as working electrodes to the completely planar control group, with all other conditions (such as CE field strength, EC potential, and distance to capillary exit) held constant. Note that the first pair of electrodes (W1AB) was shorted externally in the control group for a fair comparison with the 3D microelectrode. The electropherograms in Figure 3a demonstrate that the ECD current response increased by a factor of 1.7 for dopamine and 2.4 for catechol, respectively, at the 3D microelectrode, compared to the radial planar electrode. A computation of the signal-to-noise (S/N) ratio from the graphs yielded 19.2 for the planar electrodes while the ratio was 27.7 for the 3D microelectrodes. The elution times for both dopamine and catechol were longer, by 0.3 and 0.4 s, respectively, for the 3D LOC system, which was acceptable, considering that they were two separate microchips fabricated in different runs. Also, there was relatively more peak broadening, which was assumed to be caused by the increase in width of the 3D microelectrode, compared to the original (~30−40 μm greater). Another more obvious reason is the use of low-CE fields (50 V/cm) and, consequently, more lateral diffusion, as seen in both electropherograms. Large separation fields (>100−125 V/cm) enable faster migration as expected, but the fast speed of elution meant that the resolved current peaks were lost in the large charging current that was associated with the switch from CE to EC detection mode for the 3D electrode chips.

SEM and WYKO measurements were used to compute the fact that the change in surface area from planar to 3D was a factor of ~50 (2000 μm^2 to ~100 000 μm^2), which made the slight increase in EC current response (1.7× and 2.4×) for the two neurotransmitters perplexing. However, integration of the current over time for the electropherograms revealed the fact that there is an ~350% increase in area under the curve for the modified 3D microelectrodes. Because the area under the

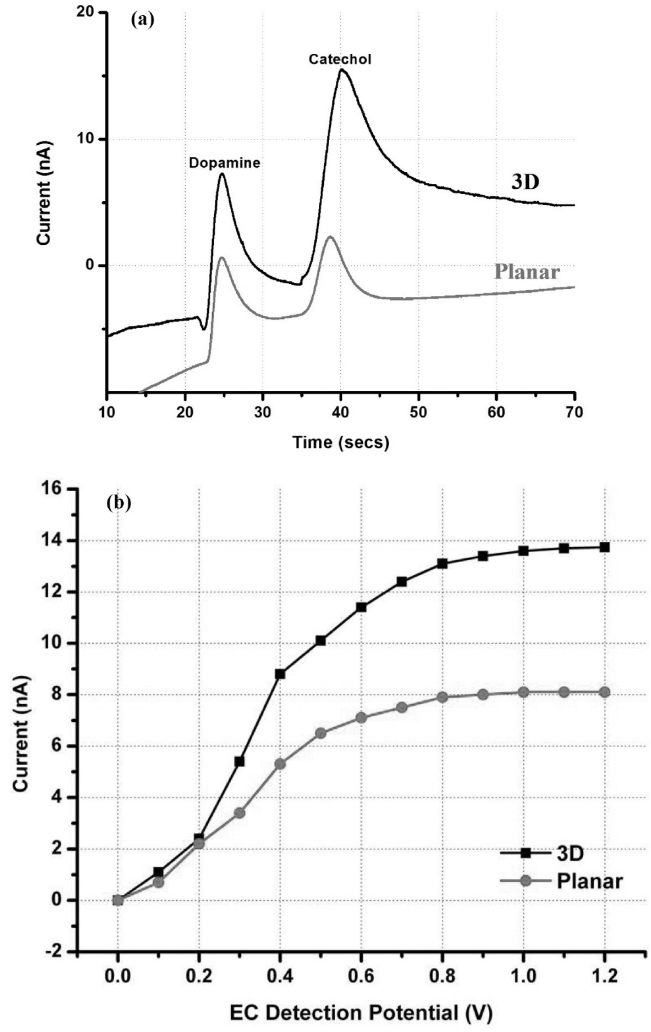

Figure 3. (a) Typical electropherograms obtained for neurotransmitters at 3D and planar electrodes, with all other conditions being the same or similar (CE = 50 V/cm; EC = 1 V; concentration = 1 mM). (b) Hydrodynamic voltammogram (HDV) comparing the 3D and planar electrodes (conditions were as follows: analyte = 1.1 mM dopamine in 0.02 M, pH 6.5 phosphate buffer, CE = 50 V/cm, EC = 0−1.2 V).

curve is proportional to the actual number of moles of the analyte being oxidized in the ECD reaction, this value was computed using the Faraday equation and compared to the total amount available, i.e., the analyte plug volume injected (~125 pL, derived from capillary dimensions and previous experiments (data not shown)). This calculation showed that the collection efficiency of the 3D electrode was 100%—i.e., all of the analyte available was being oxidized—so there could have been no more increase in signal response. Evaluation of the planar electrode's collection efficiency was performed in a similar manner and yielded values of ~34% and ~41% for the two neurotransmitters dopamine and catechol, respectively.

Furthermore, these analytical calculations were experimentally authenticated by measuring the current response at a downstream electrode poised at an oxidation potential in a dual-series EC detection scheme that is explained in the next section. Briefly summarizing, this experimental verification revealed the fact that there is no EC oxidation current at the downstream electrode due to "coulometry" or effective electrochemical removal of analyte

at the 3D electrode, whereas there was a signal in the case of the planar detection electrodes when the upstream electrodes for both planar and 3D configurations are set at an EC potential of 1 V. This data proved conclusively that the 3D electrodes, because of their higher surface area, would be "coulometric" or 100% efficient with regard to oxidizing/reducing all of the analyte available.

Hydrodynamic voltammograms (HDVs) were generated for both the 3D and planar designs (see Figure 3b) wherein the peak current for dopamine was plotted as a function of EC detection potential. Although the HDVs for both configurations exhibit "S"-curves, which is a typical characteristic of the three-electrode systems, interestingly enough, the plateau behavior that is indicative of maximum dopamine oxidation for the 3D electrode occurs at a slightly higher range of potentials (+1 V to +1.2 V), compared to the planar LOC systems (+0.8 V to +1.2 V). This fact is not only indicative of the higher-surface-area electrode having an optimal EC detection profile with a large potential range (+0.2 V to +1.2 V), but also the fact that reaction of a "volume" rather than a "plane" of analyte has significant benefits, such as higher collection efficiencies and, perhaps more importantly, coulometry, because of increased mass transfer.

As far as actual analyte quantitation was concerned, the limit of detection (S/N = 3) was determined to be 4.2 μM for dopamine and 4.3 μM for catechol at an applied potential of +1.2 V for the 3D chip, compared to the value of 17 μM that was obtained under the same conditions for a planar microchip. A linear response was observed up to 2300 μM for catechol, where y (nA) = 0.07249x + 1.094 (where x is expressed in units of μM) and R^2 = 0.9994. This performance was approximately comparable to that observed for catechols and related analytes in previous studies, especially in comparison to our own platinum electrode prototypes.[9,13] More significantly, the 4200 nM LOD for dopamine was an order of magnitude higher than the values of 100 nM and 250 nM that were obtained with 50-μm-thick platinum wire and 25-μm-thick gold wire, as reported by Liu et al.[20] However, note that, in the studies reported here, the lowest current sensitivity setting on our portable custom built EC detection system was 1 nA/V, which was a compromise that was made to gain a total operating range of ±40 nA. The range was essential to offset the background while being able to measure the increased magnitude of currents being sourced specifically because of the higher surface area in the absence of any decoupling. Therefore, the high-surface-area electrode might very well be capable of detecting lower concentrations. However, currently, the picoamp-level currents at lower concentrations cannot be measured, because of the collective compromises, such as low-sensitivity electronics, decreased CE fields, and, consequently, low mass transfer and high lateral diffusion for the higher background currents in this end-channel chip design.

Another significant difference between the nonintegrated gold and platinum wire working electrode end-channel arrangement reported by Liu et al.[20] and our study is the "coulometry" aspect. The integrated 3D microelectrode system was capable of 100% collection efficiency for the entire concentration range tested (4.3 μM to 4.4 mM (dopamine and catechol)), whereas the 50-μm-thick platinum wire in the Liu et al.[20] work was only capable of 90% collection efficiency at best and that was only for dopamine, not for catechol (~36%); Wang et al.[17] reported an LOD of 280 nM for catechol while investigating a flow-onto/flow-by carbon thick-film high-surface-area working electrode. However, this comparison to the Wang et al.[17] work would not be fair, because carbon-based detectors are known to possess better electrochemical properties than metals (such as a lower overpotential, good chemical stability, and a wider useful range). Therefore, we can say that the LOD of 4.3 μM and a separation efficiency of ~1285 for catechol (4.2 μM and 1310 for dopamine, respectively) obtained with our system are quite competitive with what has been reported in microchip studies to date. Moreover, modest changes in electronics as well as operating procedures, such as measuring LOD with high CE fields and continuous flow formats, could be implemented to increase the volume and mass transfer of analyte reactions and, consequently, obtain pM-level detection limits.

A key to the practical attractiveness of any analytical system is experimental reproducibility. The short-term repeatability studies involved repeating the same EC experiments without cleaning or refilling the reservoirs, while holding all controllable factors such as temperature, applied injection and separation voltages (CE field = 50 V/cm), EC detection potential of 1 V, etc. constant. This study showed almost-identical peak heights for both dopamine (±2.2%) and catechol (±3.7%) between successive runs. These results suggest that the system injects a very precise and repeatable volume of sample (~125 pL) and any buildup of unreacted analyte in the detection reservoir can be neglected, at least over an hour-long set of experiments. After ~1.5 h (run 30), the dopamine and catechol oxidation current peaks were 12% and 16% higher than the mean values, respectively. More emphatically, a significant tailing of the peaks or nonbaseline resolution, along with a slight increase in noise levels, was also noticed. Visual inspection of the reservoirs indicated evaporation, which, consequently, affects an increase in concentration and, hence, the resultant increase in peak heights and noise levels.

Electrode stability over time is the other important parameter for microchip devices that are intended for repeated use. The long-term studies, which were conducted over a period of days and weeks, compared results from situations where the experimental factors were the same between devices. During this time period, these LOC systems were used at least 3−4 times/week to account for a total of several hundred individual CE separations and detections. Figure 4 represents a typical collection of electropherograms spanning roughly eight months, separated on the Y-axis for better clarity. The plots for dopamine (peak height = 18.3 ± 0.7 nA, elution time = 29.4 ± 0.01 s) and catechol (peak height = 13.8 ± 0.7 nA, elution time = 44.2 ± 0.08 s) indicate that the EC detection is consistent and highly predictable. The slight variation in peak height but not in elution times may easily be attributed to the reagent solutions that were used.

During the course of this project, some devices were used in a variety of experiments with a wide range of analytes such as neurotransmitters, phenols, and metals over relatively long periods.[25,26] There was no deterioration in performance. When failure occurred, the cause was mishandling or harsh cleaning after running experiments with phenols and metals, which are two of the most difficult analytes to remove from solid metal electrodes. A chip-to-chip comparison showed slight differences in properties such as migration times (~1−2 s for similar configurations and as much as ~7 s in dissimilar chips), peak

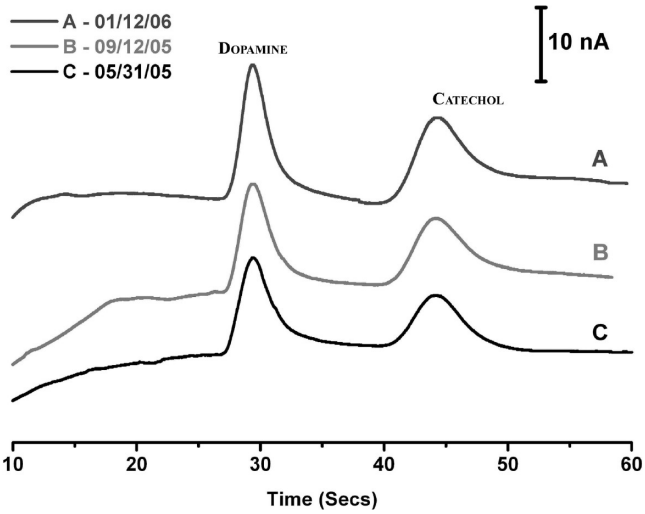

Figure 4. Electropherograms observed for 1.1 mM dopamine and catechol with the same microchip device on various dates: (A) 01/12/06, (B) 09/12/05, and (C) 05/31/05. (Conditions: CE = 50 V/cm, EC = 1 V.) [Note that a difference of 30 units has been introduced in the *Y*-axis for each graph, to ensure clarity.]

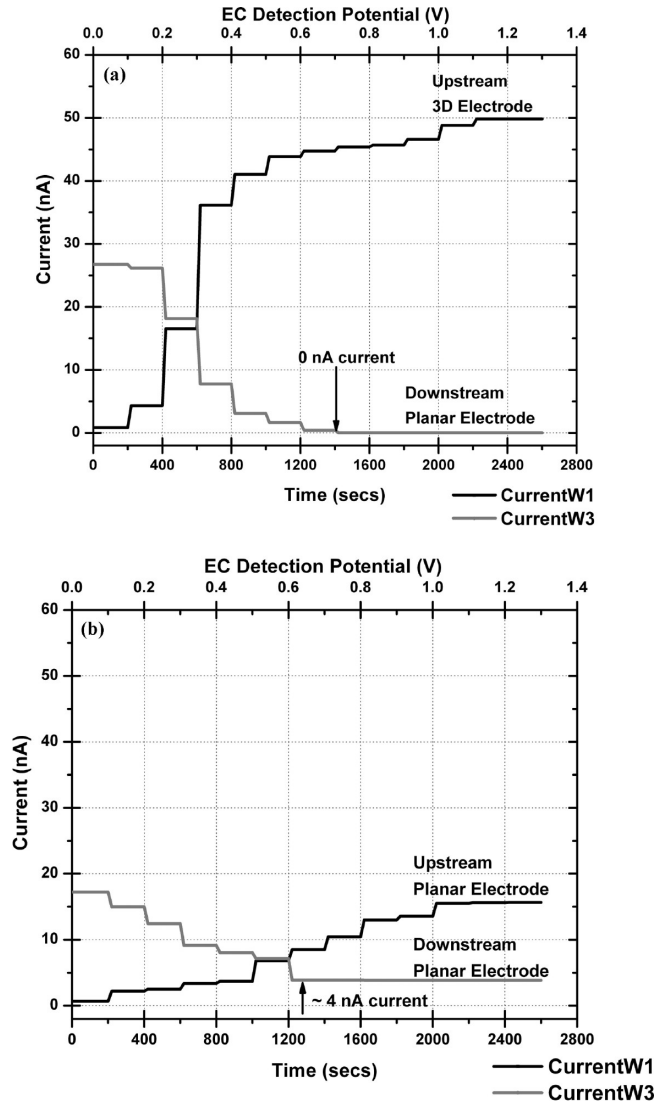

Figure 5. Experimental data demonstrating dual-series EC detection on (a) 3D and (b) planar configuration LOC systems. Conditions: analyte = 1.1 mM catechol in 0.02 M, pH 6.5 phosphate buffer; CE = 50 V/cm; EC_{W1AB} = varied from 0−1.2 V in steps of 0.1 V with EC_{W3AB} = constant, 1.0 V.

heights and widths, etc., which could be attributed to various fabrication runs and parameters; for example, the microstructure heights could be off by ±1.5 μm in a single chip (which affects the surface area), shelf widths range from 400 μm to 960 μm, and the distance from the capillary exit was variable (40−100 μm). Although the response was certainly not identical, calculations on chip performance, in terms of area under the curve and collection efficiencies using continuous flow, showed that there was ~100% coulometry at the 3D microelectrode on all 11 microchips tested. Also, the signal at the downstream electrode would be reduced to zero in both plug-flow and continuous-flow experiments in all cases at an EC potential of +0.5 V to +0.6 V. It is our belief that this consistency in the results was due to the fully integrated microchip approach used, making all the electrode positions fixed, plus the fact that a 50× increase in electrode area was achieved. Although higher concentration peaks as well as continuous-flow analyte (4.4 mM) could be removed very effectively using the 3D LOC systems, the limitation was the current range for measurement, in that the large detection currents could not be recorded with any sensitivity or range setting available in our electronics unit (±1 nA/V sensitivity for a range of ±40 nA in plug-flow format and ±10 nA/V sensitivity for a range of ±100 nA in continuous-flow format).

Dual-Series Detection. A practical application of the LOC configuration is a dual-series EC detector wherein the upstream large surface area and downstream planar electrodes could be used in conjunction for a coulometric−amperometric detection scheme, which allowed for enhancement in selectivity and sensitivity. Figures 5a and 5b demonstrate one such dual-series EC detection, comparing the amount of catechol (~1.1 mM) being oxidized to quinone on two different microchips: a 3D-planar and a planar−planar configuration (W1 and W3, respectively, in each case), with all other variables (such as shelf width, distance from capillary exit, CE field strength, etc.) being held as constant as possible between devices.

For the sake of convenience, this experiment was conducted in a continuous-flow format, where 1.1 mM catechol was streamed directly into the positive CE channel toward the detection end by operating the device in separation mode. The EC detection potential of W1 was varied in steps of +0.1 V (over a range of +0.1 V to +1.2 V) every 200 s, while keeping W3 at a constant oxidation potential of +1.0 V. Figures 5a and 5b show the oxidation current at the two detection locations on each chip (*Y*-axis), as well as the increasing detection potential applied to the first working electrode (top *X*-axis) on each chip. Each experiment was performed over the course of ~45 min, and both graphs have been derived from the mean of three runs and all currents are absolute values, as the contribution that is due to background has been measured and subtracted. Also, in both graphs, the oxidation current response plotted was the data obtained after 200 s when the system was stable. However, the individual response from each working electrode was sharp for every 0.1 V incremental adjustment. A cursory look at the electropherogram in Figure 5a indicates a much larger oxidation current at W1,

compared to that in Figure 5b, because of the increased surface area, because all other parameters were held constant. Upon further inspection of the electropherogram for the 3D LOC system, the current response at the downstream planar electrode decreases to zero at ~700 mV, indicating the complete elimination of any remaining catechol at the second working electrode (W3). Although Figure 5b shows a similar response, compared to the first experiment, incomplete oxidation of catechol in the sample stream is indicated by the remaining ~4.3 nA current at the constant 1.0 V oxidation voltage setting. This indicates incomplete removal of catechol from the flow stream by the upstream planar electrode, even at the highest oxidation voltage setting.

Confirmation of the collection efficiency for the two configurations was calculated from the experimental data on the amount of catechol oxidized compared to the total amount of catechol available in the flow stream. To summarize briefly, elution times determined by plug-flow experiments under similar conditions were used in conjunction with capillary dimensions (such as length and cross-sectional area) to compute the total amount of analyte flowing past the working electrodes for a given length of time (catechol for 200 s, in this case). The currents obtained for the different EC detection potentials were integrated over time to yield a total reaction charge, which could be converted to the amount of catechol oxidized, using Faraday's law. Approximately 30% collection efficiency was obtained at the planar working electrode, while the 3D electrode was capable of 100% collection (i.e., coulometry).

An interesting point to note is that the background current for the downstream planar electrode in Figure 5a and 5b do not both begin at the same value (~24 nA in the 3D chip, compared to 18 nA for the planar version). Because the shelf width and the distance from the capillary exit to the working electrodes was the same for both chips, it is assumed that the presence of the 3D electrode redirects some of the analyte flow to the region of the planar electrode W3, thereby allowing more sample to react initially. After the voltage is increased at the 3D electrode W1, this effect is negated. On the other hand, it might be residue from the run-to-run variations during the fabrication or the averaging that was performed to obtain the graphs. More significantly, a comparison of the results from the 3D microchips with relatively the same or similar configuration as the devices from the control group showed that this effect of higher currents on the downstream planar electrode was present in all cases, although to differing degrees (over a range of 1−8 nA).

This experiment was repeated with both microchips in a plug-flow format (data not shown). The EC potentials on the upstream electrodes were increased in steps of +0.3 V in the range of 0.0 V to +0.9 V, while keeping the downstream electrode at a constant oxidation potential of 1 V for both microchips. The main conclusions from this experiment was that the 3D LOC system exhibits a coulometric−amperometric detection scheme, because the high-surface-area electrode was capable of removing enough of the analytes dopamine and catechol when the EC potential was greater than or equal to +0.3 V, so that none reach the downstream electrode, and calculations demonstrate ~100% collection efficiency at approximately +0.9 V. On the other hand, the planar configuration can never achieve this type of collection efficiency, because there is an almost-constant signal (~4.3 nA) for both dopamine and catechol at the downstream electrode for all EC potentials. Some of the signal loss might be due to the analyte diffusion that is expected for the distance of ~235 μm between the W1 and W3 electrodes, which is compounded by the low CE separation fields (50 V/cm). Furthermore, this exact same behavior of zero measured current at the downstream electrode was determined to repeat in all of the 3D chips tested in plug-flow format (six microchips) while the control group (three devices) all showed an almost-constant residual current on the downstream electrode (data not shown). This was conclusive proof of coulometry at the 3D electrode. Perhaps more significantly, all the devices tested ($N = 11$) show 100% collection efficiency at the 3D microelectrode and only ~25%−34% conversion of catechol to quinone from the available analyte on completely planar configurations.

CONCLUSIONS

A scalable process methodology that is appropriate for the low-volume fabrication of high-surface-area microelectrodes in constrained areas for lab-on-a-chip (LOC) systems was successfully developed. In this technique, gold stud ball bumps were reshaped by imprinting with microfabricated silicon molds to create three-dimensional (3D) microarchitectures. The primary advantage of this process stems from the ability to construct multiple geometries and/or types of high-surface-area structures in one step (e.g., spirals, circles, and squares in one mold). This new alternative fabrication technique was used to construct a high-aspect-ratio/area microstructure by transforming a trio of stud bumps placed at the end of a microchannel to be used as a microelectrode (18 ± 1 μm tall, 20 μm on each side; 10 μm of spacing between adjacent micropillars) in LOC devices. Upon comparison with a control group of planar LOC systems, these fully integrated 3D microchips demonstrated 100% collection efficiency over a concentration range of 4.3 μM to 4.4 mM, and reasonable analytical performance, such as a limit of detection (LOD) of 4 μM (compared to 30% collection efficiency and a LOD of 17 μM for catechol in the planar configuration respectively), was observed. Along with these improvements in LOD and sensitivity, these microdevices exhibited consistent short-term repeatability (~60 min) and good long-term stability over eight months of continuous use. Coulometry or effective electrochemical removal via the high-surface-area electrodes in plug-flow and continuous-flow formats, as well as dual-series detection, was also demonstrated in these LOC systems; this is the first time that these two have been demonstrated successfully on a fully integrated electrochemical (EC) microchip.

ACKNOWLEDGMENT

Financial support for this work was provided by the Department of Energy (Grant No. 4-64111-01-0950) and the National Science Foundation (NSF-EPSCoR, Grant No. 4-65752-02-356). R.S.P. was funded by a University of Louisville fellowship during this project.

Received for review February 3, 2009. Accepted May 8, 2009.

AC9002529